Adv Exp Med Biol - Cell Biology and Translational Medicine (2022) 17: 227–241
https://doi.org/10.1007/5584_2022_727

Published online: 27 July 2022

Systematically Assessing Natural Compounds' Wound Healing Potential with Spheroid and Scratch Assays

Gabriel Virador, Lisa Patel, Matthew Allen, Spencer Adkins, Miguel Virador, Derek Chen, Win Thant, Niloofar Tehrani, and Victoria Virador

Abstract

Understanding cellular processes involved in wound healing is very important given that there are diseases, such as diabetes, in which wounds do not heal. To model tissue regeneration, we focus on two cellular processes: cellular proliferation, to replace cells lost to the wound, and cell motility, activated at the wound edges. We address these two processes in separate, drug responsive, in vitro models. The first model is a scaffold-free three-dimensional (3D) spheroid model, in which spheroids grow larger – to a certain extent – with increased time in culture. The second model, the scratch wound assay, is focused on cell motility. In conjunction with collagen staining, it analyzes changes to the coverage of the wound edge and wound bed. Our workflow gives insights into candidate compounds for wound healing as we show using manuka honey (MH) as an example. Spheroids are responsive to oxidative damage by hydrogen peroxide (H_2O_2) which affects viability but mostly produces disaggregation. Conversely, MH supports spheroid health, shown by size measurements and viability. In two-dimensional scratch wound assays, MH helps close wounds with relative less collagen production and increases the loose cellular coverage adjacent to and within the wound. We use these methods in the undergraduate research laboratory as teaching and standardization tools, and we hope these will be useful in similar settings.

Keywords

Collagen stain · Manuka honey · Murine stem cells · Tissue regeneration · Viability

Abbreviations

DAPI	4′,6-Diamidino-2-phenylindole
DMSO	Dimethyl sulfoxide
EDTA	Ethylenediaminetetraacetic acid
MRI	Montpellier Ressources Imagerie
MTT	3-(4,5-Dimethylthiazol-2-yl)-2,5-diphenyl-2H-tetrazolium bromide
PBS	Phosphate buffered saline
SDS	Sodium dodecyl sulfate

G. Virador
Universidad de Navarra, Pamplona, Spain

L. Patel, M. Allen, S. Adkins, M. Virador, W. Thant, N. Tehrani, and V. Virador (✉)
Montgomery College, Rockville, MD, USA
e-mail: vvirador@montgomerycollege.edu

D. Chen
Virginia-Maryland Regional College of Veterinary Medicine, Blacksburg, VA, USA

1 Introduction

The science of wound healing has its roots in the human need for survival. Since ancient times, people from all over the world have found healing substances in their environment. In general, reports of natural compounds' healing abilities are limited to case studies, while more systematic assessment of their properties is reserved for purified fractions or individual active ingredients (Atanasov et al. 2021). Generally processes of regeneration after wound are described to include hemostasis (clot formation to limit blood loss), inflammation to remove damaged cells, proliferation with formation of immature tissue (granulation tissue) and contraction of the wound, and finally, maturation of the new tissue to restore tissue functionality (Rodrigues et al. 2019). To provide an in vitro system for assessment of such natural compounds in wound healing, we have focused on two aspects of tissue regeneration: cellular proliferation in a 3D in vitro model and cell motility measured in 2D scratch wound assays. We report here our efforts to standardize a workflow for in vitro testing of candidate natural products for wound healing. Prevalent animal models in the wound healing field can be thus displaced or substituted by mini tissue models that can be generated in vitro from relevant cells and contribute important scientific insights to tissue regeneration.

Spheroids have been chosen as the model 3D systems; as such, there are thousands of publications reporting their fabrication and attempts at standardization for application to high throughput assays (Brüningk et al. 2020; Virador et al. 2019). Our spheroids are made of NIH 3T3 cells (fibroblasts, according to ATCC information) which self-aggregate in the absence of extracellular matrix or scaffold. The term fibroblast describes a broad spectrum of cellular populations which are considered mesodermal cells, are not parenchymal, and have a prominent role in generating and maintaining the extracellular matrix; however, the distinction between fibroblasts and stromal cells is unclear and more so when their murine origin is embryonic or neonate (Robey 2017). Regardless of these debates, fibroblasts are generally agreed to be precursors of various features of the mesenchyme; they can be activated in response to various signals and participate in inflammation (Buckley et al. 2001), wound healing, or cancer, by secreting growth factors and proteolytic enzymes (Kalluri 2016). The cells we used in this work are the original Swiss albino 3T3 isolated from mouse embryos by Todaro and Green (Todaro and Green 1963). While spheroids formed from the adipogenic NIH 3T3-L1 subset have been well characterized (Graham et al. 2019), there is limited information on how spheroids of the original Swiss albino cell line are formed and sustained in the absence of scaffold. Here we offer a summary of our observations on the formation of these spheroids which appears to be chiefly dependent on the plastic surface and well size.

We established a reproducible workflow to form spheroids in a 96-well format, as well as time and end points to screen for natural compounds for wound healing. By testing cell viability as an end point, we intended to find compounds which consistently increased spheroid viability in a set time. These compounds would then be taken to the well-established scratch wound healing assay in 2D to verify their ability to increase the cell motility needed to close the wound. We added collagen staining of the 48-h wounds to our procedure to demonstrate whether the compound increases or decreases collagen production. In our analysis of scratch wounds, we looked at the traditional ratio of wound closure, but we also included the analysis of the loose space around the wound, providing insight on potential effects of the compound on cellular subpopulations affected by the wound. As an example of our workflow applied to a natural compound, we present results obtained with MH, a kind of honey native to New Zealand, produced by bees which pollinate the manuka bush flower (*Leptospermum scoparium*) and for which there are many reports showing positive effects in wounds (Tashkandi 2021).

2 Materials and Methods

2.1 Cells and Culture Conditions

The cells we used in our experiments are NIH 3T3 fibroblasts (CCL-92, ATCC, Manassas, VA). Cells were expanded and multiple vials were kept frozen under liquid nitrogen. A set of experiments was conducted from one expanded vial. Cells were used for a low number of passages (typically less than 7). Cells were monitored for mycoplasma contamination by visually assessing DAPI (4′,6-diamidino-2-phenylindole) stained samples. For regular culture maintenance and to expand cells for 3D experiments, cells were grown in T75 flasks in DMEM with high glucose, supplemented with 10% v/v bovine calf serum and 1% penicillin-streptomycin, at 37° C in a humidified atmosphere with 5% CO_2. Flat bottom 96-well plates (Corning, NY) were used for monolayer cell viability tests and flat bottom 12-well plates (Corning, NY) for scratch wound assays. For 3D spheroids, polystyrene round bottom low adhesion plates (Greiner Bio1, Cat 650,970, Monroe, NC) or non-tissue culture treated polystyrene flat well multiwell plates (VWR, 10861–556 or 10,861–558) were used, and similar sized tissue culture treated polystyrene flat well plates were used for comparison (e.g., CELLTREAT Scientific Products, Pepperell, MA).

2.2 Spheroid Formation for Compound Screening

Subconfluent cells with more than 90% viability as assessed by Trypan Blue staining were passaged with a 0.48 mM EDTA in PBS rinse (VERSENE, ThermoFisher, Waltham, MA) and exposure to 0.25% Trypsin/EDTA. Cells were centrifuged at 700 RPM for 5 min and resuspended in fresh media before seeding onto various surfaces as detailed in figure legends. In round bottom low adherence 96-well plates, 50,000 cells per well in 50 μl media were seeded. Outer wells contained only 100 μl of PBS. When spheroids had formed (typically by day 3 after seeding), 50 μl media containing the test compounds were added to each well. Cultures were monitored daily, and viability was assessed by adding MTT at the end of 1 week.

2.3 Dissolving Natural Compounds: Spheroid Treatment

MH, a product of New Zealand, was purchased from Costco (Y.S Eco Bee Farms, Sheridan, IL LOT # 9178 – the same lot was used throughout the project), and a stock solution of 1 g/ml was prepared as follows: first, 4 g of MH were weighed and dissolved in 1 ml of deionized water. The stock vial was kept at 37 °C for a few hours to overnight. When the honey stock was a fine suspension/solution, the total volume was assessed, and then the final solution was diluted with deionized water to a final concentration of 1 g/ml (w:v). From this stock solution, half-log dilution series was prepared with deionized water.

Commercially available 3% hydrogen peroxide from a freshly opened bottle was used to produce a half-log dilution series using deionized water. Care was taken to use a very small volume of each compound stock to produce final concentrations in spheroid medium.

When spheroids had formed (typically by day 3 after seeding), 50 μl media containing the test compounds were added to each well. This brought the total volume in well to 100 μl. Cultures were monitored daily.

2.4 Cell Viability and Stains

The MTT reduction assay (Berridge and Tan 1993) was used as follows: each well containing one spheroid received 10 μl MTT (Sigma-Aldrich, St. Louis, MO) dissolved in water to a final concentration of 0.5 mg/ml MTT. The spheroids were incubated at 37 °C and 5% CO_2 for 45 min, and then solubilizing reagent (10% SDS in 0.01 M HCl) was added. The plate was

maintained overnight at room temperature in the dark after which the amount of MTT formazan formed was measured at 450 nm in a Tristar2 Multimode Reader LB942 (Berthold Technologies, Oak Ridge, TN).

Mito tracker green (Molecular Probes) was dissolved in DMSO and added to the cultures at a 100 nM final concentration for 15 min in incubator prior to fixing.

Rhodamine-phalloidin (Molecular Probes) was dissolved in methanol and added to the cultures at nanomolar concentration according to manufacturer's recommendation. DAPI (Invitrogen) was dissolved in deionized water and added to the cultures according to manufacturer's recommendation.

Mason Trichrome stain to detect collagen in scratch wound assays was done as follows: Forty-eight hours post scratch, after documenting the live cell culture, cells were fixed with 4% paraformaldehyde, and then the protocol http://www.ihcworld.com/_protocols/special_stains/masson_trichrome.htm was followed.

2.5 Scratch Wounds

Subconfluent NIH 3T3 cells were seeded in 24-well plates at 10000 cells per well. Prior to seeding, a line was drawn on the underside of the wells to facilitate recording the same location of the wound over time. Two days later, medium was removed and a scratch was made by gliding a 100 µl pipette tip vertically through the center of the well, followed by a PBS rinse to eliminate floating debris and addition of media containing the test compounds. Pictures were taken immediately (time 0) at 24 and 48 h to document scratch reduction.

2.6 Imaging and Measurements

Fluorescence images were taken in an EVOS M5000 microscope with a highly sensitive 3.2 MP monochrome CMOS camera (2048 × 1536) with 3.45-µm pixel resolution (Thermo Fisher). For brightfield images, an EVOS XLCore (AMEX 1000, Invitrogen) was used. To measure spheroids, using brightfield or phase contrast, the focus was adjusted so that the images represented a circular cross section of the spheroid at its center, with the diameter of the circle matching that of the spheroid.

For scratch wounds, images were taken in the same area of each wound using the previously drawn marker and the wound as reference. The MRI Wound Healing plugin for ImageJ/Fiji® was used to analyze scratch wound images using the variance method (filter radius, 10; radius open, 4; min size, 10,000) https://github.com/MontpellierRessourcesImagerie/imagej_macros_and_scripts/wiki/Wound-Healing-Tool.

Original images, converted to 8-bit images, were used as input and processed with a fixed threshold value of 20 to find the area that contained no cells. Adjusting the selection threshold in the plugin settings up to a fixed threshold number of 100 allowed for distinction between empty space and loose cellular coverage. Ratio of closure was calculated by dividing the area given by ImageJ (in pixels) at the specific time by the area at time 0 in the same well.

To quantitate large cells, present in the wound area, ImageJ "analyze particles" plugin was used on 8-bit images with size (100-infinity) and circularity (0.50–1.00) settings. These settings were adopted after comparing the data obtained with results obtained by visual counting.

2.7 Histology

Spheroids were fixed in 4% paraformaldehyde (Electron Microscopy Sciences, Hatfield, PA) for 15 min, rinsed with PBS, and carefully placed between lens paper and then embedded and sectioned using routine protocols (summarized in https://www.corning.com/catalog/cls/documents/protocols/CLS-AN-431_DL.pdf). Hematoxylin- and eosin-stained sections were imaged in an EVOS XLCore microscope at 10 x magnification.

2.8 Statistics

Experiments had an N = 3 (three independent experiments) with six to eight biological replicates per condition unless indicated. Data were analyzed with Microsoft Excel and with

GraphPad Prism software (GraphPad, San Diego, USA). All the statistical analyses were performed with GraphPad Prism. Data are reported as mean ± SD *$p < 0.05$, **$p < 0.01$, ***$p < 0.0001$.

3 Results

3.1 NIH 3T3 Spheroids Self-Assemble from Cell Sheets in the Absence of Extracellular Matrix

CCL-92 is a 3T3-Swiss albino embryonic cell line from *Mus musculus*, house mouse, which grows as adherent monolayers on flat tissue culture surfaces. In 24-well non-tissue culture treated polystyrene plates, cells formed spontaneous clusters of varied shapes ranging from small colonies (between 100 and 200 μm in diameter) to larger spheroids (300 and 800 μm in diameter depending on plate and time in culture). We compared morphological stages of these spontaneous clusters and timing in various flat bottom plates. For example, at day 10 after plating, the non-tissue culture treated plate (VWR) had formed small colonies in 6 out of 24 wells, spheroids in 7 out of 24 wells, and stretched ribbons in 5 wells, while the remaining 6 wells contained small pieces of cell sheet curling at the edges. Sarstedt flat bottom tissue culture plate showed similar adhesions and pulling sheets which took longer to detach, and only fragments of cell sheets or flat sheets with ruffled edges were observed at day 10. In tissue culture treated plates with special adhesion properties for difficult to grow cells, for example, CELLTREAT, the pulling from the edges was observed in 15/24 wells, but the cell sheets never completely detached and sheet or cell clusters did not form even after 3 weeks in culture (Fig. 1a, top panels), while various shaped tissue clusters appeared in the VWR non-tissue culture plate in the same time frame (Fig. 1a, bottom panels). Most of the larger spontaneous clusters had tubular morphologies, and some resembled incomplete toroids. Detailed observation of the stages of cluster formation indicated that 2D compact cell sheets formed in various regions of the plate with one or more strong adhesions to the edges of the plate or to each other (Fig. 1b). In cases when the compact sheets had a stronger attachment to the plate, the edges curled (Fig. 1c), but in most cases complete rolling of the sheet edges occurred to form spheroids or pouches or wells filled with colonies and small spheroids (Fig. 1d). In some cases, adhesions on symmetrical ends of the cell sheet stretched and rolled over small colonies engulfing them (Fig. 1e). These observations agree with a recent report (Granato et al. 2017) of spontaneous clusters formed by human dermal myofibroblasts. Histology of typical tissue aggregates indicates that they possess a thick wall and some have a lumen (Fig. 1f–i).

Since it appeared that all different tissue aggregates formed in a similar fashion, we focused on documenting the formation of small spheroid pouches in 96-well round bottom plates. For reproducible spheroids, we found it was very important to put the plate after seeding on a flat surface at room temperature absent of any vibration, before putting it into the incubator, which is also proposed as a technique to reduce edge effect (Lundholt et al. 2003; White et al. 2019). First, we used Costar 7007 plates, made of ultralow attachment polystyrene. In these plates, the spheroids did not appear to go through the process of folding but appeared spheroidal in shape from the day of seeding. These spheroids had an average size of 0.15 mm^2 at day 12 with an increase to 0.19 mm^2 at day 15 and a progressive decrease to 0.17 mm^2 by day 23 consistent with spheroid maturation (Graham et al. 2019). Based on these observations, we speculate that spheroids made in those ultralow attachment plates may be similar to those made from cancer cells described as a "closely packed, spherical geometry of cells" (Mueller-Klieser 2000), but they do not appear to have undergone sheet retraction and folding.

We screened other 96-well polystyrene plates and found that CellStar suspension plates produced tissue structures from cell sheets. By observing the same well at days 4, 5, and 7 post seeding, we could document that spheroid formation begins by folding, rolling, and finally detaching from symmetrical stress fiber adhesions

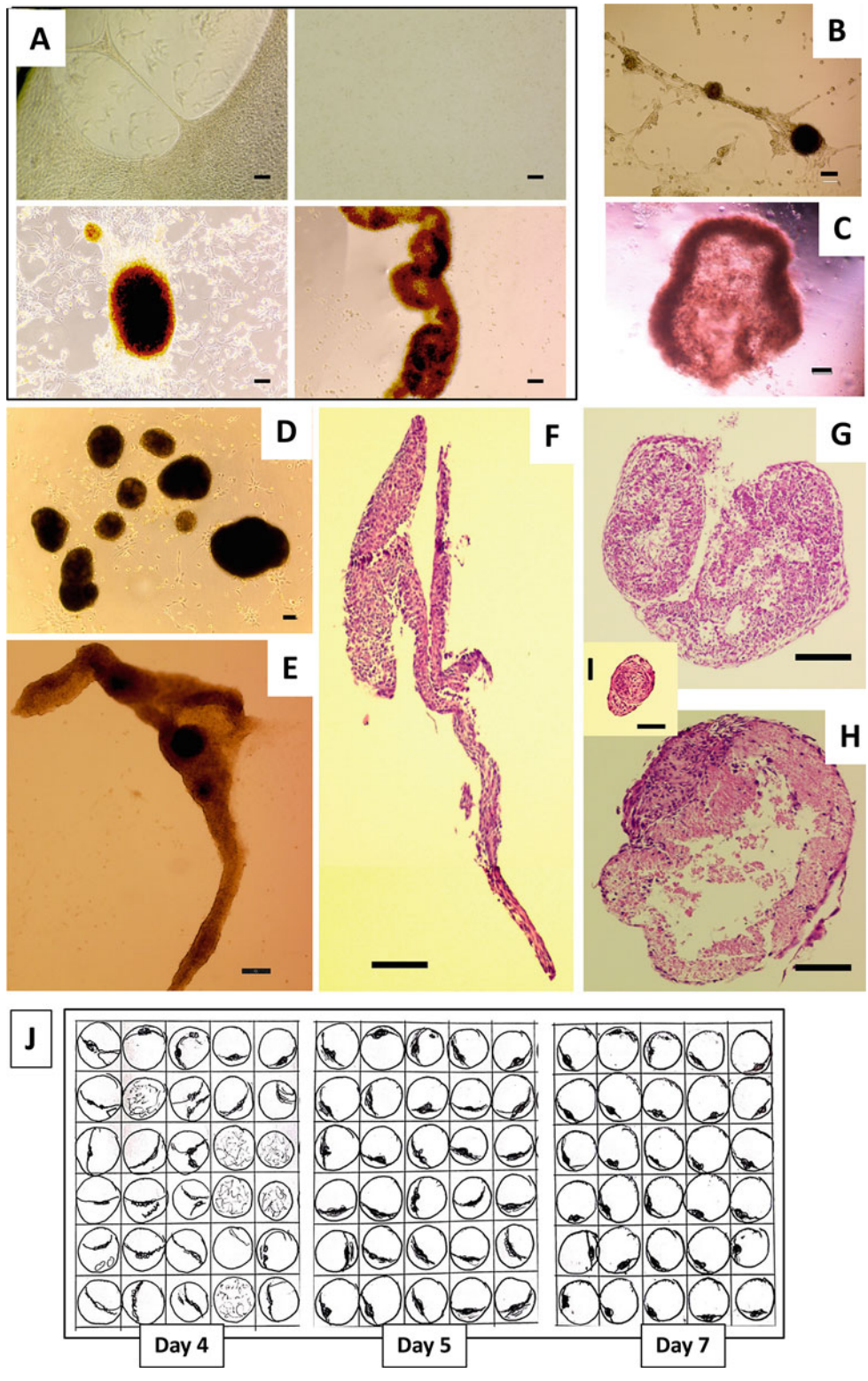

Fig. 1 Examples of tissue aggregates from cell sheets formed in low adhesion plates
(**a**) Three-week-old cultures of NIH3T3 cells (CCL92). Top panels show cells grown in CELLTREAT plates, left image shows the edge of the plate where sheets start pulling away, and right image shows tightly attached

to the concave well edges, thus undergoing similar stages to the non-tissue culture 24-well plates (Fig. 1j). Then, increased stretching was accompanied by rolling of the sheet like a candy wrapper, prior to formation of the spheroid, which resembled the closing of a pouch. In a small percentage of cases, flat sheets with ruffled edges were also observed in the 96-well plate due to imperfect pouch formation. Of note, these observations and drawings were part of a "Introduction to Scientific Research" class in a community college setting aimed at familiarizing students with cell biology and fostering scientific curiosity and systematic scientific skills.

3.2 Manuka Honey Is a Spheroid-Supporting Compound

To standardize 3D assays for multiwell plates, spheroids are preferred as they are more regular in size and reproducible. In preliminary experiments using MTT, we determined that 1-week treatment of spheroids without a medium change does not significantly alter their viability (data not shown) possibly because, once formed, spheroids have low metabolic activity compared with cells that are actively dividing (Granato et al. 2017; Fukushima et al. 2019).

Once we could reliably produce spheroids in 96-well plate and characterize their growth, we focused on standardizing methods to assess natural compounds reported as wound healing aids, many of which are part of botanical complex mixtures. To assess drug responsiveness of our model, we first chose H_2O_2, to induce oxidative stress (Sies 2017), and we compared its effect on confluent monolayers and on spheroids (Fig. 2a, b, c). As expected, the decrease of viability in response to H_2O_2 was more pronounced in monolayers. After testing a new candidate compound in monolayer, we proceeded to test spheroid drug responsiveness by assessing viability in a standardized manner in 96-well round bottom plates as shown in Fig. 2d.

Next MH with its antioxidant, antibacterial (Carter et al. 2016), and wound healing properties (Bulman et al. 2017; Frydman et al. 2020; Mokhtar et al. 2020; White 2016) was chosen to test our workflow. We found that when MH was present in the culture from the time of cell seeding (in a range of concentrations from 0.3 to 100 mg/ml), spheroids formed by day 3 in 60% of the wells compared to 20% in its absence. From this early data, we concluded that MH was a spheroid-supporting compound, whereas H_2O_2 was a spheroid-damaging compound, and this was supported by the viability data (Fig. 2e) where H_2O_2 produced a small but consistent decrease in viability while MH produced a dose-dependent small but consistent increase in viability suggesting a small increase in proliferation (Fig. 2f). Our observations indicated that spheroids responded to oxidative damage by initially disassembling, consistent with oxidative stress effects on tight junctions (Gangwar et al. 2017). Interestingly, spheroids were able to reassemble similarly to the findings of (Brüningk et al. 2020), and this reassembly was prevented by a second addition of H_2O_2 (data not shown). We speculate that this ability to reassemble may be one of the reasons for the more limited

Fig. 1 (continued) monolayer. Bottom panel, examples of cell clusters formed in wells of VWR non-tissue culture treated plates. (**b**) Colonies are formed as cell clusters pull away from each other. (**c**) An incomplete spheroid formed by rolling the edges of a flat sheet. (**d**) Small colonies and spheroids 200–500 μm in diameter. (**e**) Several colonies formed on a sheet are enveloped as the sheet rolls and gathers. (**f**) Hematoxylin-eosin stained section of a long cluster with tubular end. (**g,h**) Hematoxylin-eosin stained sections of typical 500 μm spheroids. (**i**) Hematoxylin-eosin stained section of a small 200 μm colony. (**j**) Detailed drawings of spheroid formation in 96-well low adhesion plate containing 50,000 cells per well; the same well is drawn at day 4, 5, and 7 post seeding. Scale bars, 100 μm

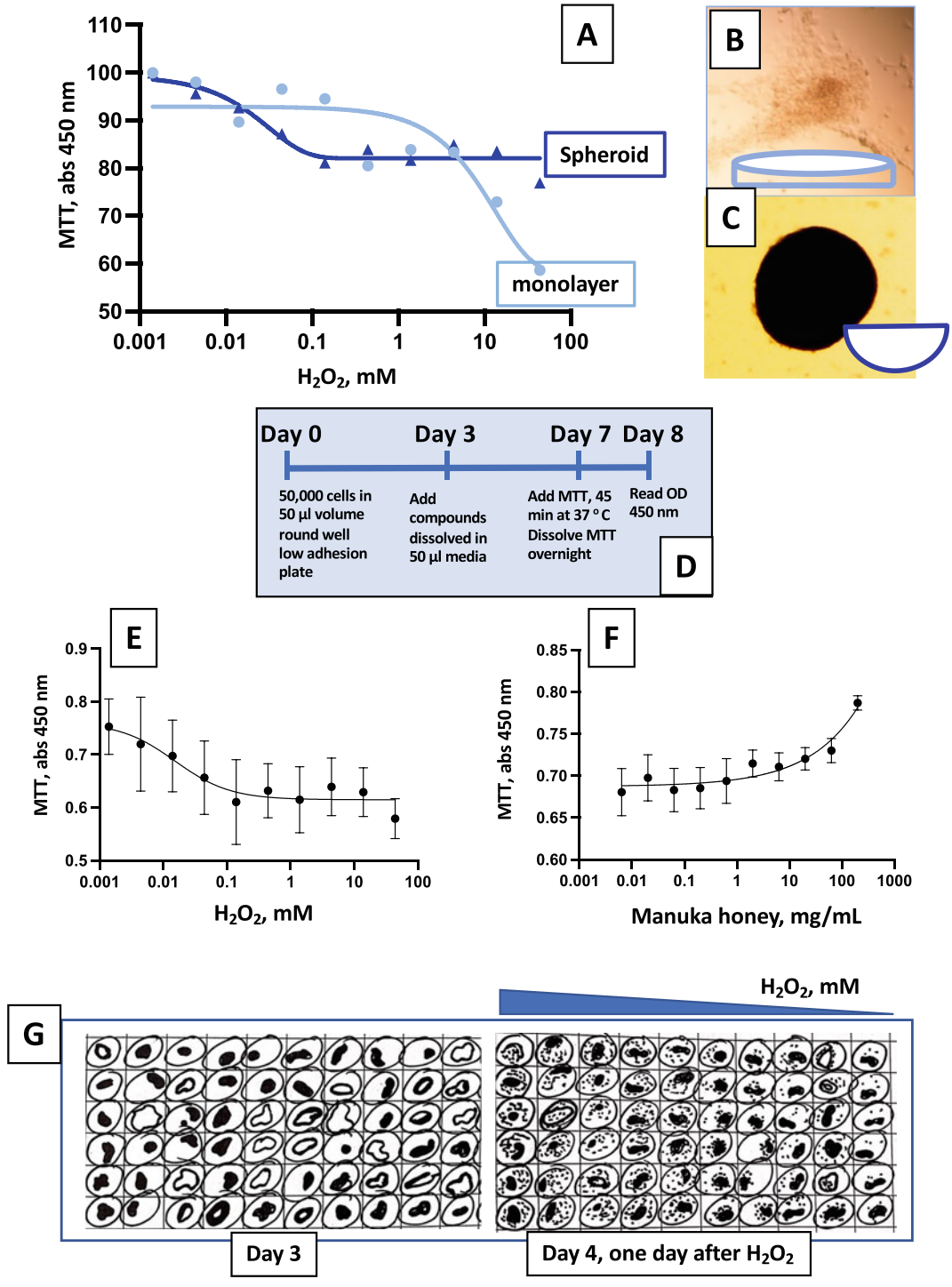

Fig. 2 Spheroids are responsive to drug treatments Response of confluent monolayer of 10,000 cells per well (light blue line and panel B) vs. spheroids (dark blue line and panel C) to increasing concentrations of H_2O_2. D. Standardized treatment scheme applied to spheroids for all compounds tested. E. Cell viability in response to H_2O_2 treatment measured by MTT absorbance (450 nm). F. Cell viability in response to MH treatment measured by MTT absorbance (450 nm). Summary data from three independent experiments with six technical replicates for each concentration. G. H_2O_2 causes disaggregation of the spheroids. Left panel, spheroid plate at day 3 prior to adding H_2O_2; right panel, spheroid plate at day 4, after 24 h of addition of H_2O_2 at the same concentrations as shown in panel E

decrease in viability observed when comparing to H_2O_2 treated monolayers.

Next, we measured spheroid surface area at several concentrations of H_2O_2 and MH. We found that at low H_2O_2 concentrations when viability is decreasing, spheroids have smaller sizes than control (Fig. 3a, b), but at higher than 0.1 mM spheroids actually became bigger, perhaps due to swelling or to different patterns of shrinkage and regrowth as seen in other studies (Brüningk et al. 2020). For MH we found a small but consistent increase in spheroid size at the concentrations we tested (Fig. 3c, d).

3.3 Manuka Honey Increases Cell Motility in Scratch Wound Assays

After MH had been established as a spheroid-supporting compound, we used the scratch wound assay to investigate the compound's effect on cell motility. Our method to produce and document the scratch wounds was adapted from (Pinto et al. 2019). Scratch wound assays are typically analyzed by segmenting the images with imaging programs to document and quantitate the amount of closure of the wound in a given amount of time, generally 24 h. For example, the MRI wound healing plugin is extensively cited in these studies (Kauanova et al. 2021). Basically, the method highlights different areas in the image by replacing each pixel with the specified neighboring area through a variance filter with a specific radius to effectively differentiate the aspect of tissue from the empty areas (also see (Suarez-Arnedo et al. 2020)). These studies generally look for disappearance of the empty space in the wound bed. Using ImageJ plugin "MRI wound healing tool" to follow the decrease in empty space in the presence of MH, we found no significant difference (Fig. 4a).

We realized that analyzing the images of the empty space did not provide sufficient

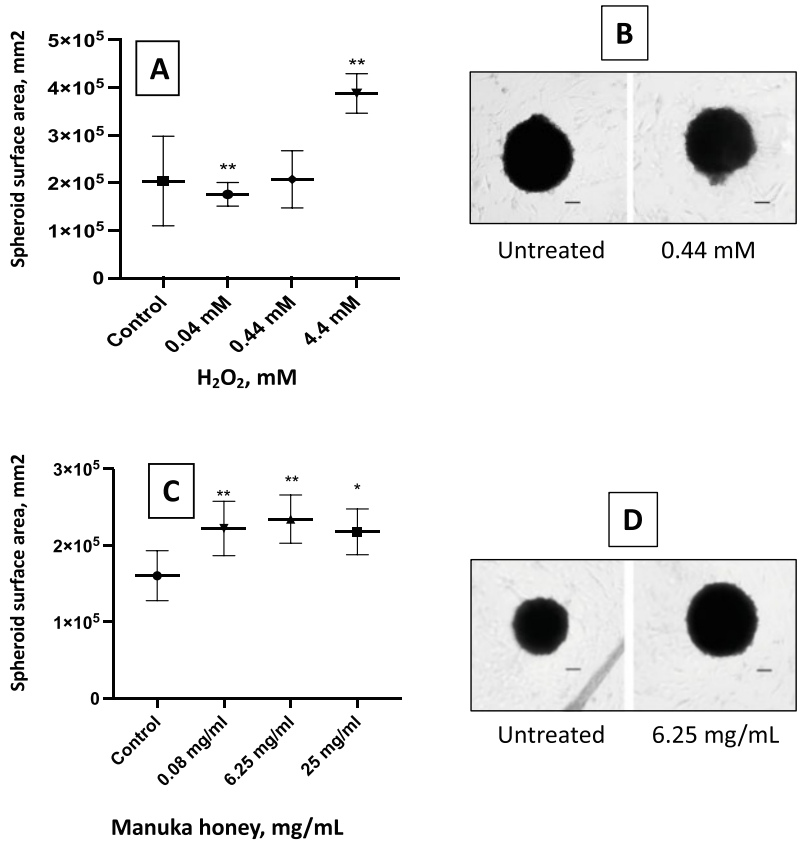

Fig. 3 MH is a spheroid-supporting compound (**a**) Size change in spheroid in response to H_2O_2. (**b**) Representative spheroid pictures taken at day 7 of the treatment protocol left spheroid control, right spheroid with 0.44 mM H_2O_2. (**c**) Size change in spheroid in response to MH. (**d**) Left spheroid control, right spheroid with 6.25 mg/ml MH. Experiments were carried out twice with six technical replicates per concentration, and one representative experiment is shown

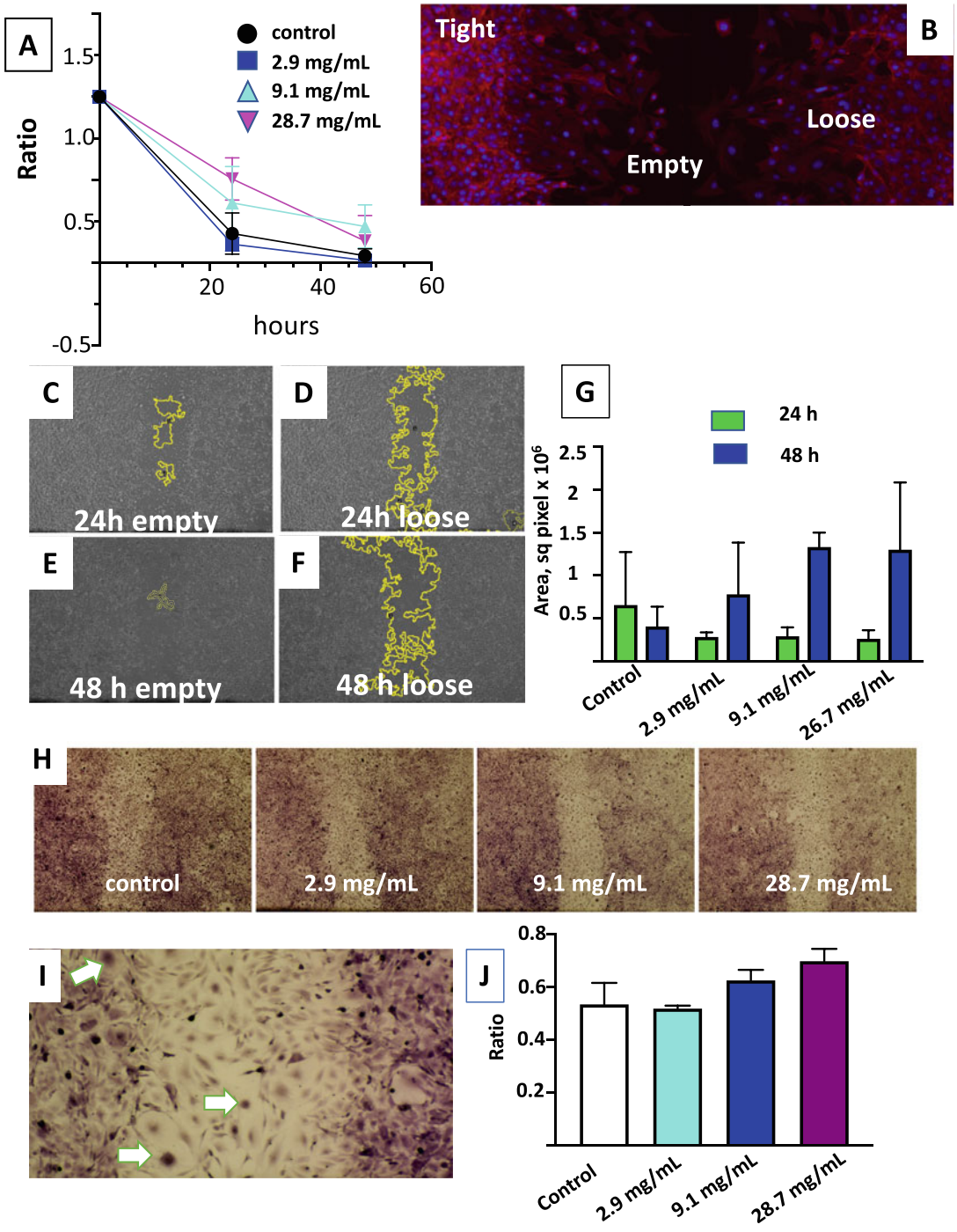

Fig. 4 Scratch wound assays treated with MH (**a**) Closure of the wound, ratio of empty space (treated vs. control) at 24 and 48 h post wound. Unpaired t test, NS. (**b**) Rhodamine-phalloidin stained wound demonstrating three kinds of cellular coverage: empty, loose, and tight. (**c**) Cellular coverage quantified with ImageJ MRI wound healing tool by assigning fixed thresholds to each image; as example, 24-h scratch treated with 2.9 mg/ml honey, threshold 20 to quantify empty space. (**d**) Twenty-four-hour scratch treated with 2.9 mg/ml honey, threshold 100 to quantify loose space. (**e**) Forty-eight-hour scratch treated with 2.9 mg/ml honey, threshold

information regarding the closure of wounds because the wound margin did not completely disappear at 24 h or even at 48 h in our experiments, and this margin was clearly noticeable when we stained for collagen; therefore, we looked for alternative ways to analyze our images which could provide insights as to what effects the compound might have on the complex processes occurring around and within the wound.

With the MRI wound healing plugin, we first tried to divide the images into three regions based on visual assessment of their morphology which correlated with the pixel density obtained from ImageJ; we could thus distinguish between empty space; loose coverage, characterized by motile cells; and the remaining tight coverage, denser cellular coverage surrounding empty and loose coverage. In other words, loose-empty space represents visual culture heterogeneity away from the homogeneous tight space (Fig. 4b). As we saw no significant change in the tight coverage at 24 h, we focused on analyzing empty and loose coverage by the ImageJ variance method after choosing two thresholds that were representative of empty space and loose space (Fig. 4c–f). Next, we followed the empty and loose space at 24 and 48 h post wound with various concentrations of MH, and we found there was a trend toward increased loose space with MH treatment at 48 h (Fig. 3g), indicating an increase in culture heterogeneity. We wondered if that correlated with an increase in fibrotic cells and stained for collagen in the 48-h wounds. Interestingly, our results suggest that MH does not increase collagen but rather decreases it (Fig. 4h–i), and this supports recent reports of scarless healing with MH (Singh et al. 2018).

We wondered what cells could contribute to the measured increase in loose space and turned our attention to flat giant cells, which appear to be interpreted by the MRI tool as empty space within covered space. These may be myofibroblast precursor cells, or perhaps fibrocytes (Reilkoff et al. 2011; Tomasek et al. 2002), mesenchymal cells with features both of fibroblasts and macrophages involved in tissue remodeling. Visual assessment and quantitation of flat giant cells in scratch wound images within and outside the wound area using ImageJ suggested that the number of such cells increases in MH treated scratch wounds, particularly in the wound area.

Taken together, our results presented here give added quantitative evidence to qualitative and anecdotal studies of MH applications in human wound healing.

4 Discussion

4.1 Scaffold-Free Spheroids from NIH 3T3 Cells Form by Substrate-Specific Collective Cellular Processes from Cell Sheets

There are different forms of 3D cellular aggregates broadly grouped under the terms "spheroids" and "organoids" (a very good current review of the nomenclature is found in (Decarli et al. 2021)). Both kinds of aggregates may form spontaneously in culture from cellular populations which contain a large proportion of stem cells or early progenitors. Organoids, characterized by their ability to organize in a manner similar to their tissue of origin, usually contain multiple cell types (Clevers 2016); they arise in tissue culture either by disaggregation of tissues and limited culturing or from coaxing stem

Fig. 4 (continued) 20 to quantify empty space. (**f**) Forty-eight-hour scratch treated with 2.9 mg/ml honey, threshold 100 to quantify loose space. (**g**) Loose minus empty space for each MH concentration. (**h**) Collagen staining 48 h post scratch in MH treated wounds. (**i**) Flat giant cells observed within and outside the margins of the wound. (**j**) Ratio of flat giant cells occupying the space within the wound to total flat giant cells in the image after 48 h. Data are representative of at least two independent experiments with three technical replicates per condition

cells into aggregation by modifications of their environment. The term spheroid is reserved for multicellular spherical shaped clusters of cells from homogeneous cell populations or cell lines of various tissue origins. Such cellular aggregates clump together and maintain their spherical shape with or without exogenous extracellular matrices. For difficult to culture cells, various scaffolds made of hydrogel materials are required (Caliari and Burdick 2016). The spheroids we describe here are very similar in their appearance to those shown by (Granato et al. 2017) formed using human dermal cells aggregated in hanging drops and collected in agarose coated plates, whereas our spheroids form and are maintained in the absence of scaffold. Similar to spheroids from cancer cell lines, commonly used in 3D screens for drug discovery, which are relatively easy to form and maintain scaffold-free, our spheroids are also good models for 3D screens because the absence of scaffold decreases complexity and variability for the screen. This study adds to the relatively scarce literature characterizing spheroid cultures with fibroblasts in the absence of hydrogel materials (Jorgenson et al. 2017; Graham et al. 2019).

It is clear that the stages of formation of spheroids differ greatly among various cell types (Smyrek et al. 2019; Livoti and Morgan 2010) and particularly if one compares cancer line derived spheroids to those originated from progenitor populations. Our work sheds light into a specific mode of formation of stem cell derived spheroids from collective rolling of cell sheets which is highly dependent on interaction with the surface. Using sarcoma cells on polyacrylamide substrates (Beaune et al. 2018) observed cell sheet collective behavior to be highly dependent on surface rigidity. We report here that, only using low adhesion plates, the stages of spheroid formation consisted of the production of a thin layer of cells spreading through the surface which pulled and broke in various places in the same time frame (roughly within 1 min) to produce a collective rolling edge of cells that quickly gathered to a pouch to close a spheroid if the surface area was small. With the same kind of adhesion and increased surface area, the stages of aggregate formation were similar but produced varied shapes and sizes.

4.2 Using Spheroids and Scratch Wound Healing Assays to Screen Natural Compounds

Botanical complex mixtures have been used since ancient times to heal minor wounds and scratches. Despite many hurdles to the research and development of natural compounds, there is renewed interest in their therapeutic potential, especially as sources for new antimicrobial treatments. Important considerations when characterizing natural compounds are their difficult solubility and availability to the cells in culture, the inherent difficulties in bioactive compound isolation and in elucidating its cellular target (Atanasov et al. 2021), and the fact that synergisms between various components with beneficial therapeutic outcomes (Schmidt et al. 2007) may obscure the contribution of a component in the mixture to the overall bioactivity of a natural compound.

We start characterization of spheroid-supporting or spheroid-disrupting compounds by measuring cell viability with the colorimetric MTT assay. The use of this method is not without controversy due to low reproducibility (Stepanenko and Dmitrenko 2015), but, in our experience, it serves didactic purposes. Our students visualize cellular activity under the microscope after a few minutes' incubation, and they also learn to collect colorimetric data and, more importantly, learn to appreciate the differences between monolayers and spheroids (Fig. 2a). Even though it is currently accepted that 3D in vitro models are superior to monolayers in drug screening, it is harder to find the most relevant end point to assess bioactivity (White et al. 2019). In our case, since we have characterized the formation of the spheroids, preventing formation via oxidative stress and supporting it with compounds such as MH, we are now in the position to set up screening for compounds that facilitate pulling and rolling of sheet edges to aid spheroid formation and support its stability.

Scratch assays are relatively simple assays that have provided important information about cell motility and have been used for drug screening. However, more information can be gained from more sophisticated image analysis as others have recently shown (Kauanova et al. 2021). Our image analysis focuses on measuring the clearly different region near and within the wound that is covered by highly motile cells. This phenomenon is useful as a unit of study because its speed of formation and cellular components can be altered by the presence of natural compounds such as MH.

There is some controversy in the literature as to whether or not spheroids may be fibrosis models. Some argue they are, because they can contain activated myofibroblasts (Kisseleva 2017), whereas others (Granato et al. 2017; Avagliano et al. 2019) suggest that spheroids are not fibrosis models because the myofibroblasts within them become deactivated and that their formation closely resembles the physiological modes of skin wound healing. Spheroids from dysregulated transcriptional coactivator with PDZ-binding motif (TAZ) grow more than normal (Jorgenson et al. 2017), and these could be considered a model of fibrosis. Our results with spheroids formed with NIH 3T3 cells support Granato's conclusions suggesting our spheroids are physiologically stable since (a) acidification of the media does not happen in spheroid containing wells while it happens in actively growing monolayers (our unpublished observations) and (b) there is no significant change in spheroid size after 2 weeks in culture. Though we have yet to ascertain the reason for some increase in size of the spheroids with MH, this change does not seem to be due to increased ECM production (collagen) because in our scratch wound assays, visually the amount of collagen accumulated in cells nearing the wound was less in MH treated wounds in accordance with a recent report of scarless wound healing with MH (Singh et al. 2018). Our analyses of the scratch wounds also uncovered the possible contribution of flat giant cells to the increased loose coverage with MH treatment. It is possible that MH increases the number and proliferation of these cells which may be proto myofibroblasts (Tomasek et al. 2002; Avagliano et al. 2019) or fibrocytes (Reilkoff et al. 2011). We still do not know the nature of these large cells, just that they are part of the loose coverage, and our future work will address this.

4.3 Usefulness of Our Proposed Workflow

With the workflow presented here, we can get insights on cellular events that may be modified by a wound healing compound. This can be useful for further characterization of the compound; similar to MH, other compounds that produce a moderate increase in viability can then be taken to the scratch assays in 2D to verify their ability to increase the cell motility needed to close the wound. In our analysis of scratch wounds, we look at the traditional ratio of wound closure, but we also include the analysis of the loose space around the wound, providing insight on potential effects of the compound on cellular subpopulations affected by wound. We added collagen staining of the 48-h wounds to our workflow to demonstrate whether the compound increases or decreases collagen production as a readout for fibrosis.

There are many case reports or anecdotal reports about natural compounds used in wound healing, many of which are based on animal testing, while our workflow uses in vitro systems that do not rely on animal testing.

Finally, we use these methods to teach cell biology and introduction to research to undergraduate students with very limited experience in the lab. The workflow was established as a collaborative effort among the students in a low budget setting. We hope these methods can be adopted and expanded in similar settings.

Acknowledgments This work has been supported by Montgomery College, SCIR 297 program, and by support from Schoenberg Fellowship to V.V. We are thankful to Lauren Kimlin and to Greta Babakhanova for their help with the ImageJ analyses and for the constant assistance and support of Arifur Rahman, Ya Yu Shao, and Chris Standing, our lab staff.

Contributions G. V. performed experiments, analyzed data, and reviewed the manuscript; M. A. analyzed data and prepared figures; L. P., S. A., M. V., D. C., W. T., and N. T. performed experiments and analyzed data; and V. V. conceived the studies, performed experiments, analyzed data, and wrote the manuscript. All authors read and approved the manuscript.

References

Atanasov AG, Zotchev SB, Dirsch VM et al (2021) Natural products in drug discovery: advances and opportunities. Nat Rev Drug Discov 20:200–216. https://doi.org/10.1038/s41573-020-00114-z

Avagliano A, Ruocco MR, Nasso R et al (2019) Development of a stromal microenvironment experimental model containing proto-myofibroblast like cells and analysis of its crosstalk with melanoma cells: a new tool to potentiate and stabilize tumor suppressor phenotype of dermal myofibroblasts. Cell 8. https://doi.org/10.3390/cells8111435

Beaune G, Blanch-Mercader C, Douezan S et al (2018) Spontaneous migration of cellular aggregates from giant keratocytes to running spheroids. Proc Natl Acad Sci U S A 115:12926–12931. https://doi.org/10.1073/pnas.1811348115

Berridge MV, Tan AS (1993) Characterization of the cellular reduction of 3-(4,5-dimethylthiazol-2-yl)-2,5-diphenyltetrazolium bromide (MTT): subcellular localization, substrate dependence, and involvement of mitochondrial electron transport in MTT reduction. Arch Biochem Biophys 303:474–482. https://doi.org/10.1006/abbi.1993.1311

Brüningk SC, Rivens I, Box C et al (2020) 3d tumour spheroids for the prediction of the effects of radiation and hyperthermia treatments. Sci Rep 10:1653. https://doi.org/10.1038/s41598-020-58569-4

Buckley CD, Pilling D, Lord JM et al (2001) Fibroblasts regulate the switch from acute resolving to chronic persistent inflammation. Trends Immunol 22:199–204. https://doi.org/10.1016/s1471-4906(01)01863-4

Bulman SEL, Tronci G, Goswami P et al (2017) Antibacterial properties of nonwoven wound dressings coated with manuka honey or methylglyoxal. Materials (Basel) 10. https://doi.org/10.3390/ma10080954

Caliari SR, Burdick JA (2016) A practical guide to hydrogels for cell culture. Nat Methods 13:405–414. https://doi.org/10.1038/nmeth.3839

Carter DA, Blair SE, Cokcetin NN et al (2016) Therapeutic manuka honey: no longer so alternative. Front Microbiol 7:569. https://doi.org/10.3389/fmicb.2016.00569

Clevers H (2016) Modeling development and disease with organoids. Cell 165:1586–1597. https://doi.org/10.1016/j.cell.2016.05.082

Decarli MC, do Amaral, R. L. F., Dos Santos, D. P. et al (2021) Cell spheroids as a versatile research platform: formation mechanisms, high throughput production, characterization and applications. Biofabrication. https://doi.org/10.1088/1758-5090/abe6f2

Frydman GH, Olaleye D, Annamalai D et al (2020) Manuka honey microneedles for enhanced wound healing and the prevention and/or treatment of methicillin-resistant staphylococcus aureus (mrsa) surgical site infection. Sci Rep 10:13229. https://doi.org/10.1038/s41598-020-70186-9

Fukushima T, Tanaka Y, Hamey FK et al (2019) Discrimination of dormant and active hematopoietic stem cells by g0 marker reveals dormancy regulation by cytoplasmic calcium. Cell Rep 29(4144–4158):e4147. https://doi.org/10.1016/j.celrep.2019.11.061

Gangwar R, Meena AS, Shukla PK et al (2017) Calcium-mediated oxidative stress: a common mechanism in tight junction disruption by different types of cellular stress. Biochem J 474:731–749. https://doi.org/10.1042/BCJ20160679

Graham AD, Pandey R, Tsancheva VS et al (2019) The development of a high throughput drug-responsive model of white adipose tissue comprising adipogenic 3t3-l1 cells in a 3d matrix. Biofabrication 12:015018. https://doi.org/10.1088/1758-5090/ab56fe

Granato G, Ruocco MR, Iaccarino A et al (2017) Generation and analysis of spheroids from human primary skin myofibroblasts: an experimental system to study myofibroblasts deactivation. Cell Death Disc 3:17038. https://doi.org/10.1038/cddiscovery.2017.38

Jorgenson AJ, Choi KM, Sicard D et al (2017) Taz activation drives fibroblast spheroid growth, expression of profibrotic paracrine signals, and context-dependent ECM gene expression. Am J Physiol Cell Physiol 312:C277–C285. https://doi.org/10.1152/ajpcell.00205.2016

Kalluri R (2016) The biology and function of fibroblasts in cancer. Nat Rev Cancer 16:582–598. https://doi.org/10.1038/nrc.2016.73

Kauanova S, Urazbayev A, Vorobjev I (2021) The frequent sampling of wound scratch assay reveals the "opportunity" window for quantitative evaluation of cell motility-impeding drugs. Front Cell Dev Biol 9:640972. https://doi.org/10.3389/fcell.2021.640972

Kisseleva T (2017) The origin of fibrogenic myofibroblasts in fibrotic liver. Hepatology 65:1039–1043. https://doi.org/10.1002/hep.28948

Livoti CM, Morgan JR (2010) Self-assembly and tissue fusion of toroid-shaped minimal building units. Tissue Eng Part A 16:2051–2061. https://doi.org/10.1089/ten.TEA.2009.0607

Lundholt BK, Scudder KM, Pagliaro L (2003) A simple technique for reducing edge effect in cell-based assays. J Biomol Screen 8:566–570. https://doi.org/10.1177/1087057103256465

Mokhtar JA, McBain AJ, Ledder RG et al (2020) Exposure to a manuka honey wound gel is associated with changes in bacterial virulence and antimicrobial susceptibility. Front Microbiol 11:2036. https://doi.org/10.3389/fmicb.2020.02036

Mueller-Klieser W (2000) Tumor biology and experimental therapeutics. Crit Rev Oncol Hematol 36:123–139. https://doi.org/10.1016/s1040-8428(00)00082-2

Pinto BI, Cruz ND, Lujan OR et al (2019) In vitro scratch assay to demonstrate effects of arsenic on skin cell migration. J Vis Exp. https://doi.org/10.3791/58838

Reilkoff RA, Bucala R, Herzog EL (2011) Fibrocytes: emerging effector cells in chronic inflammation. Nat Rev Immunol 11:427–435. https://doi.org/10.1038/nri2990

Robey P (2017) "Mesenchymal stem cells": fact or fiction, and implications in their therapeutic use. F1000Res 6. https://doi.org/10.12688/f1000research.10955.1

Rodrigues M, Kosaric N, Bonham CA et al (2019) Wound healing: a cellular perspective. Physiol Rev 99:665–706. https://doi.org/10.1152/physrev.00067.2017

Schmidt BM, Ribnicky DM, Lipsky PE et al (2007) Revisiting the ancient concept of botanical therapeutics. Nat Chem Biol 3:360–366. https://doi.org/10.1038/nchembio0707-360

Sies H (2017) Hydrogen peroxide as a central redox signaling molecule in physiological oxidative stress: oxidative eustress. Redox Biol 11:613–619. https://doi.org/10.1016/j.redox.2016.12.035

Singh S, Gupta A, Gupta B (2018) Scar free healing mediated by the release of aloe vera and manuka honey from dextran bionanocomposite wound dressings. Int J Biol Macromol 120:1581–1590. https://doi.org/10.1016/j.ijbiomac.2018.09.124

Smyrek I, Mathew B, Fischer SC et al (2019) E-cadherin, actin, microtubules and fak dominate different spheroid formation phases and important elements of tissue integrity. Biol Open 8. https://doi.org/10.1242/bio.037051

Stepanenko AA, Dmitrenko VV (2015) Pitfalls of the MTT assay: direct and off-target effects of inhibitors can result in over/underestimation of cell viability. Gene 574:193–203. https://doi.org/10.1016/j.gene.2015.08.009

Suarez-Arnedo A, Torres Figueroa F, Clavijo C et al (2020) An image j plugin for the high throughput image analysis of in vitro scratch wound healing assays. PLoS One 15:e0232565. https://doi.org/10.1371/journal.pone.0232565

Tashkandi H (2021) Honey in wound healing: an updated review. Open Life Sci 16:1091–1100. https://doi.org/10.1515/biol-2021-0084

Todaro GJ, Green H (1963) Quantitative studies of the growth of mouse embryo cells in culture and their development into established lines. J Cell Biol 17:299–313. https://doi.org/10.1083/jcb.17.2.299

Tomasek JJ, Gabbiani G, Hinz B et al (2002) Myofibroblasts and mechano-regulation of connective tissue remodelling. Nat Rev Mol Cell Biol 3:349–363. https://doi.org/10.1038/nrm809

Virador GM, de Marcos L, Virador VM (2019) Skin wound healing: refractory wounds and novel solutions. Methods Mol Biol 1879:221–241. https://doi.org/10.1007/7651_2018_161

White R (2016) Manuka honey in wound management: greater than the sum of its parts? J Wound Care 25:539–543. https://doi.org/10.12968/jowc.2016.25.9.539

White JR, Abodeely M, Ahmed S et al (2019) Best practices in bioassay development to support registration of biopharmaceuticals. BioTechniques 67:126–137. https://doi.org/10.2144/btn-2019-0031